



Broad-band tunable visible emission of sol–gel derived SiBOC ceramic thin films

Aylin Karakuscu^{a,*}, Romain Guider^b, Lorenzo Pavesi^b, Gian Domenico Sorarù^a

^a Department of Materials Engineering and Industrial Technology, Engineering Faculty-University of Trento, 38050 Trento, Italy

^b Nanoscience Laboratory, Department of Physics-University of Trento, 38050 Povo, Trento, Italy

ARTICLE INFO

Article history:

Received 7 May 2010

Received in revised form 7 January 2011

Accepted 11 January 2011

Available online 27 January 2011

Keywords:

Photoluminescence

Sol-gel

External quantum efficiency

Boron

Borosilicates

ABSTRACT

Strong broad band tunable visible emission of SiBOC ceramic films is reported and the results are compared with one of boron free SiOC ceramic films. The insertion of boron into the SiOC network is verified by Fourier-Transform Infrared Spectroscopy. Optical properties are studied by photoluminescence and ultraviolet-visible spectroscopy measurements. Boron addition causes a decrease in the emission intensity attributed to defect states and shifts the emission to the visible range at lower temperatures (800–900 °C) leading to a very broad tunable emission with high external quantum efficiency.

Published by Elsevier B.V.

1. Introduction

Polymer pyrolysis is a processing method for complex Si–O–C, Si–C–N, and Si–(E)–O–C E=B, Al, Ti, Zr,... ceramic systems which cannot be synthesized via other methods [1]. Ternary SiOC ceramics, also called silicon oxycarbide glasses, are obtained from siloxanes, through pyrolysis in inert atmosphere at a temperature exceeding 800 °C [2,3].

Cross-linked polysiloxanes or silicon resins can be prepared by the sol–gel process through hydrolysis and condensation reactions of hybrid silicon alkoxides [4]. The sol–gel process allows a precise control of the composition of the starting silicon resin by co-hydrolyzing different hybrid silicon alkoxides. Moreover, extra elements such as Al, Ti or B can be homogeneously introduced in the preceramic network via the corresponding metal alkoxides [5,6].

The ceramic nanostructure, which evolves step-by-step from the polymer precursors, consists of a random network built up by mixed SiO_{4-x}C_x 0 ≤ x ≤ 4 units with excess carbon forming sp² graphene layers [7]. This disordered structure forms at a relatively low temperature (800–1000 °C) and rearranges at a higher temperature (1200–1400 °C) leading to a nanostructured ceramic consisting of two interpenetrating silica-rich and C-rich networks with a dispersion of nanocrystalline SiC [7].

Nowadays, Polymer Derived Ceramics (PDCs) belonging to the Si–O–C as well as the Si–C–N system attract much attention by their intense photoluminescence (PL) [8,9]. In the literature, several

promising results on bulk [10], powders [8,9] and thin films [11,12] have been reported. However, the origin of the photoluminescence in PDCs is still a matter of discussion among the scientific community. While in some studies the emitted light has been associated with the formation of dangling bonds and sp² C atoms during pyrolysis [8], others researchers explained the PL origin by precipitation of sp² C clusters into an amorphous Si_xC_yO_zH_w [11] and lately, the intense photoluminescence observed for an amorphous siliconoxycarbonitride ceramic has been attributed for the presence of mixed bonds of Si–C–N–O tetrahedra [9]. Recent studies in our group have shown that the photoluminescence behaviour of SiOC-based thin films and their emission wavelengths can be tuned over the visible range by changing the chemical composition and pyrolysis temperature [12,13]. At low pyrolysis temperatures (800–1000 °C), a blue emission band is observed, which has been ascribed to defects in the amorphous network such as C dangling bonds; while at higher temperatures, 1000–1250 °C, a broad band emission dominates the luminescence. The origin of this behaviour at high temperatures has been attributed to phase separation of the amorphous SiOC network leading to the formation of optically active Si, SiC and C clusters [12].

Boron addition to silicon oxycarbide glasses is known to accelerate the phase partitioning and SiC crystallization [14,15]. Moreover, boron decreases the free carbon amount in the SiBOC ceramic by forming new B–C bonds and increases the complexity of the amorphous network by forming mixed boron oxycarbide units, BO_{3-y}C_y 0 ≤ y ≤ 3 [14,15]. Therefore, the formation of emitting centers in the SiBOC system could be favoured and may occur at lower temperatures. In this work, we studied the photoluminescence behaviour of SiBOC films with the aim to control the luminescent behaviour of SiOC films more efficiently through boron addition.

* Corresponding author.

E-mail address: aylin.karakuscu@ing.unitn.it (A. Karakuscu).

2. Experimental details

SiBOC thin films are produced by the sol-gel method using a mixture of triethoxysilane (T^H) and methyl-diethoxysilane (D^H) with a T^H/D^H molar ratio of 2 to obtain silicon oxycarbide with a negligible amount of free C [16]. Triethylborate (TEB), $B(OCH_2CH_3)_3$, is used as a source of boron and was added to the silicon solution to obtain a B/Si ratio of 0.1. Ethanol was used as solvent and the hydrolysis was promoted adding acidified water. Thin films, which we labelled TEB- $T^H D^H 2$, are deposited on Si and SiO_2 substrates by spin coating and then pyrolysed in a carbon furnace under Ar flow at temperatures in a range of 800–1200 °C. Results were compared with boron free SiOC films, $T^H D^H 2$, prepared from the same sol-gel precursor solution without triethylborate addition.

3. Characterization techniques

The surface and morphological feature of the SiBOC films were investigated by Jeol JSM-5500 Scanning Electron Microscopy (SEM). Operating voltage is kept at 10 kV for all analysis. The surface qualities and roughness of the films were investigated by NT-MDT P47H semi-contact mode Atomic Force Microscopy (AFM) operating with NSC12-MikroMasch noncontact ultrasharp silicon cantilever tip. Film thicknesses were determined by using a Hommel tester T8000 profilometer. The bonding structure of the films, gels and pyrolysed samples, was investigated by Fourier-Transform Infrared Spectroscopy (FTIR). Nicolet Avatar 330 FTIR was used in transmission mode to follow the structural evolution with increasing pyrolysis temperature for films on the Si substrate.

Photoluminescence measurements (PL) were recorded at room temperature using a double monochromator DMS-2, SOPRA spectrometer. The samples were excited by an Argon Laser (365 nm) with 0.1 mW power on the sample. PL intensities were normalized to follow the evolution of the emission through the pyrolysis process. In addition to PL spectra, External Quantum Efficiency (EQE) were analysed to investigate the potential of the films. The transmission and reflectance spectra of the TEB- $T^H D^H 2$ films were recorded over the region 190–800 nm using a Carry 3, UV-Vis spectrophotometer.

4. Results and discussion

Homogeneous and crack free films at every pyrolysis temperature are achieved by adding a drying stage before pyrolysis. The effect of this step can be seen in the SEM and AFM images of the films pyrolysed at 1200 °C, shown in Fig. 1. Without drying, large cracks covered the film surface (Fig. 1a); these cracks completely disappeared only after keeping the films at 80 °C for 24 h before pyrolysis. This additional drying stage also helped to obtain low roughness values. AFM analysis of the pyrolysed SiBOC films (Fig. 1b) gave an average roughness of 2.8 nm, similar to SiOC films [17].

FTIR spectra recorded on the as coated films are shown Fig. 2. B–O stretching absorption at around 1400 cm^{-1} confirmed the presence of boron in the structure [18]. Si–H bonds of T^H units gave rise to absorptions at: 2243 cm^{-1} (ν) and 831 cm^{-1} (δ), while those of D^H units led to the band at 2173 cm^{-1} (ν). The Si–H absorptions in the two films were very similar suggesting that the introduction of triethylborate into to the T^H/D^H solution did not cause any preferential hydrolysis of the Si–H bonds. The Si– CH_3 (ν) at 1261 cm^{-1} and at 760 cm^{-1} (rocking), and Si–O stretching band in a range of 1140 – 1065 cm^{-1} were the same in both samples. In conclusion, the addition of TEB to the sol-gel solution allowed introducing boron into the structure preserving the Si–H functionalities of the T^H/D^H precursors. This is an important result because Si–H moieties are required to efficiently incorporate C into the SiOC network during the pyrolysis. The lack of Si–H may cause abundant C cluster formation

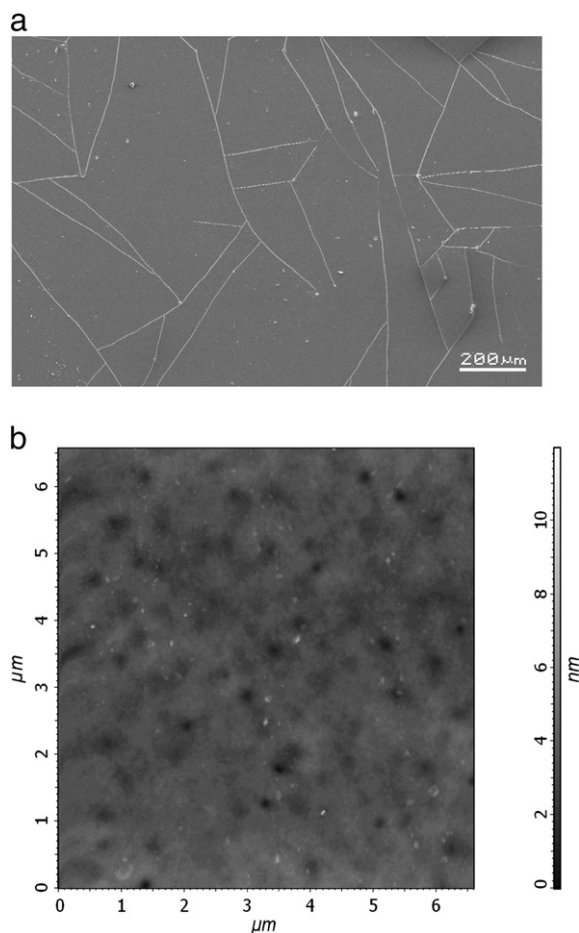


Fig. 1. (a) SEM and (b) AFM images of SiBOC films annealed at 1200 °C before and after the optimization, respectively.

and produce a completely non-transparent black glass [16], which is unwanted in our case.

FTIR spectra of the films pyrolysed at 1100 °C are reported in Fig. 3. The band at 1400 cm^{-1} and the shoulder at 560 cm^{-1} were assigned to B–O (ν) and O–B–O (δ) respectively [6] and prove that boron is retained in the pyrolysed films. The main band at around 600 cm^{-1} is originated from the substrate (Si–Si). In both spectra bands at 1140 – 1065 cm^{-1} (Si–O stretching) and at 800 cm^{-1} (Si–C) were present suggesting the formation of a silicon oxycarbide glass [19]. The

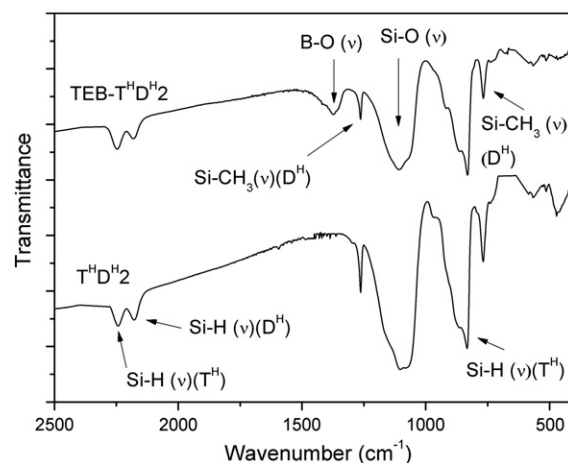


Fig. 2. FTIR spectra of as-coated TEB- $T^H D^H 2$ and $T^H D^H 2$ films. The boron related band is indicated.

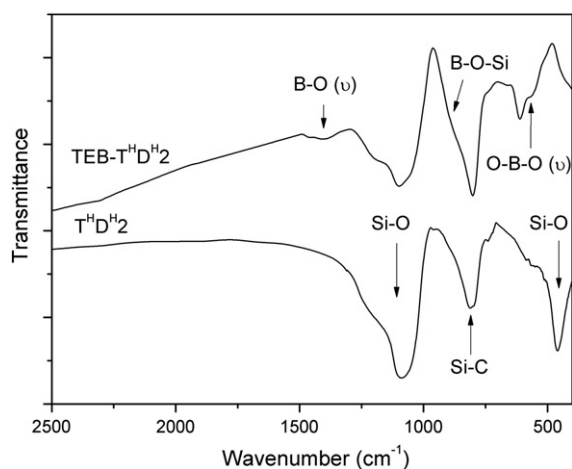


Fig. 3. FTIR spectra of TEB- $T^H D^H_2$ and $T^H D^H_2$ films pyrolysed at 1100 °C. Corresponding bands are indicated.

intensity of the Si-C bond is considerably higher and narrower in the TEB- $T^H D^H_2$ film, which may be due to a higher in concentration of Si-C bonds and/or a more ordered structure. Moreover, the shoulder at 915 cm^{-1} can be assigned to the presence of $\equiv\text{Si-O-B}\equiv$ bridges revealing the homogeneous incorporation of boron into the silica-based network [20].

The evolution of the thickness during pyrolysis is followed by profilometer measurements. The thicknesses of the as coated films were close to each other (see Table 1). As the temperature increases, TEB- $T^H D^H_2$ films shrank less than $T^H D^H_2$ leading to thicker films at 1100 °C (Table 1). The linear shrinkage of the TEB- $T^H D^H_2$ after pyrolysing at 1100 °C was 36% which is essentially lower than $T^H D^H_2$ films (45%). This result must be related with the higher ceramic yield of the B-containing system compared to the B-free gel. Indeed, it is known that addition of B to $T^H D^H$ gelling solutions allows getting ultra-high ceramic yield, up to 97 wt.% [21].

Photoluminescence spectra of TEB- $T^H D^H_2$ films show very interesting features (Fig. 4a). A very broad emission starting from 410 nm (3 eV) can be seen in the PL spectrum of the sample pyrolysed at 800 °C. The emission peak radically shifts to green–yellow range at 900 °C by preserving its extremely wide line-shape. Please note that this emission peak covered all visible range as well as UV and IR region ($<400\text{--}850\text{ nm}$). Further increase in the pyrolysis temperature caused a continuous PL peak shift towards yellow–orange and then red range, while the line-shape still maintains its broadness. Photographs of the TEB- $T^H D^H_2$ films pyrolysed at 800–1100 °C under a UV lamp are shown in Fig. 5. Films pyrolysed at temperatures higher than 1100 °C gave emission outside the detectable limits and therefore they were not reported. In order to understand the PL origin of the SiBOC films, we compare them with B-free SiOC films.

The photoluminescence spectra of $T^H D^H_2$ films are shown in Fig. 4b and they are quite different than those of TEB- $T^H D^H_2$ films proving the strong effect of B on the PL behaviour of SiBOC films. At 800–1000 °C, the SiOC PL spectra are dominated by a principal component in the UV range at 400–450 nm, which has been assigned to defect states such as C dangling bonds [12]. This peak can only be

Table 1

Thickness values for as-coated and films pyrolysed at 1100 °C and calculated linear shrinkage values.

Films	Thickness		Linear Shrinkage at 1100 °C
	As-coated	1100 °C	
$T^H D^H_2$	910 μm	490 nm	45% \pm 3
TEB- $T^H D^H_2$	980 μm	640 nm	36% \pm 3

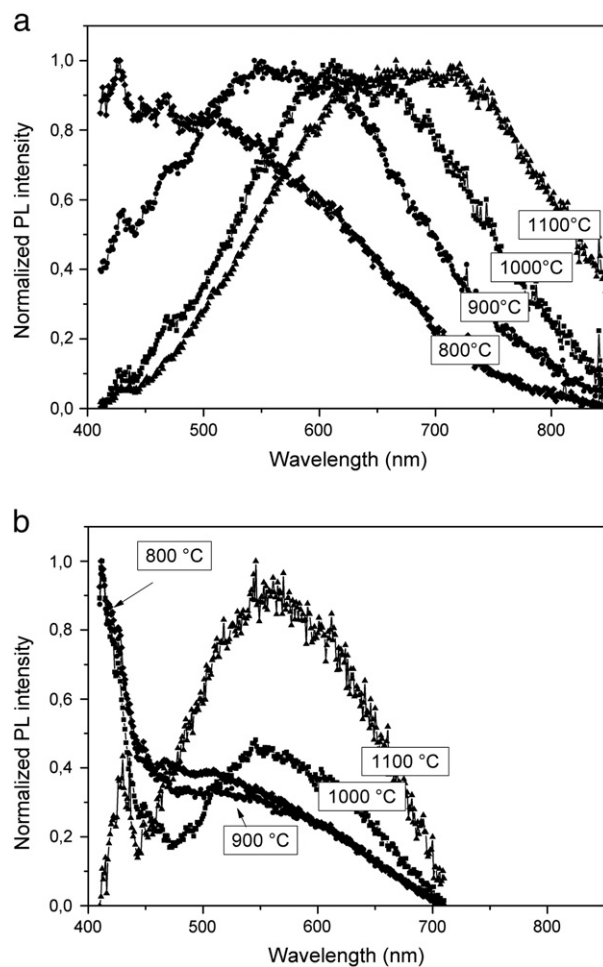


Fig. 4. Normalized photoluminescence spectra of the (a) TEB- $T^H D^H_2$ and (b) $T^H D^H_2$ thin films pyrolysed at temperatures in a range of 800–1100 °C.

seen at low temperatures ($\leq 1000\text{ °C}$) and it vanishes at higher temperatures following a trend similar to the concentration of C dangling bonds as reported for PDC systems [22]. On the other hand, this main peak is not present in TEB- $T^H D^H_2$ films. The absence of the UV peak in TEB- $T^H D^H_2$ films suggests that C radicals do not form in high amount in this system or if they form, they are consumed faster than in the B-free system. In fact, it is known that during pyrolysis boron reacts with C to form new B-C bonds and this may reduce the development of C radicals [14,23]. Unfortunately, in the FTIR spectra there is no evidence for the formation of B-C bonds. This is not surprising since, based on our previous studies on SiBOC glass powders prepared from the same sol-gel-derived precursor, the presence of mixed boron oxycarbide units, $\text{BO}_{3-x}\text{C}_x$ was detected only by ^{11}B MAS NMR analysis and no absorption bands were seen in the corresponding FTIR spectra [23]. Therefore, we believe that formation of B-C bonds in the studied SiBOC films is highly probable and they may contribute in reducing the development of C radicals and the corresponding UV-light emission.

As the pyrolysis temperature increases, both TEB- $T^H D^H_2$ and $T^H D^H_2$ films tend to give visible luminescence. $T^H D^H_2$ films pyrolysed at 1000 °C showed a new peak at around 560 nm and this peak became the principal emission for samples pyrolysed at 1100 °C without showing any red-shift. At this pyrolysis temperature, the UV peak is strongly reduced and emission is centered in the green–yellow range. The origin of the green–yellow PL peak in the SiOC films has been previously discussed and assigned to the presence of SiC and C clusters [12]. This visible emission is achieved at a lower temperature (900 °C) in TEB- $T^H D^H_2$ films. At this pyrolysis temperature, extremely

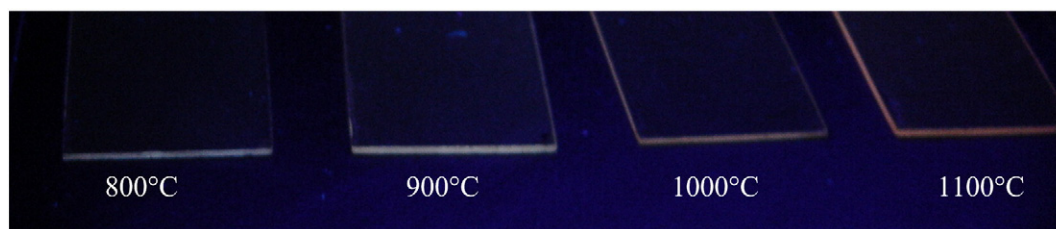


Fig. 5. Photograph of the TEB- $T^H D^H_2$ thin films pyrolysed from 800 to 1100 °C under UV laser excitation.

broad emission compared to the boron free film, is clearly visible in Fig. 4.

The PL of samples pyrolysed at high temperatures reveals two main differences between TEB- $T^H D^H_2$ and $T^H D^H_2$ films: the emission line-width and the spectral shift. PL emission of the TEB- $T^H D^H_2$ films reaches a width of 290 nm at 1100 °C with a significant red shift compared to the $T^H D^H_2$ films. Such a broad emission could be assigned to the simultaneous presence of multiple emitting centers. SiBOCs are expected to be more complex than ternary SiOCs since they contain not only mixed silicon oxycarbide units, (SiC_xO_{2-x} , $0 \leq x \leq 4$) and sp^2 C clusters, but also boron oxycarbide units (BC_yO_{3-y} , $0 \leq y \leq 3$). Thus, the origin of the wide PL emission observed in TEB- $T^H D^H_2$ films could be ascribed to multiple emitting centers of the complex SiBOC network as well as to the presence of SiC and C clusters with a wide

size distribution (as for the ternary SiOC films). Moreover, the red shift observed in TEB- $T^H D^H_2$ films could be related to the evolution of the amorphous SiBOC structure with the pyrolysis temperature, which is known to occur at lower temperatures when B is inserted into the inorganic network compared to the pure ternary SiOC [14,15].

The transmittance spectra of the TEB- $T^H D^H_2$ and $T^H D^H_2$ films are shown in Fig. 6a. Transmittance decreased with increasing the pyrolysis temperature. The film pyrolysed at 800 °C was almost totally transparent for almost all visible colours (≥ 420 nm). An increase in the pyrolysis temperature caused a red shift as well as a decrease in transparency. The optical absorption edge was below 200 nm for all films. The oscillations in the graphs which were well evident for the sample pyrolysed at 800 °C are due to the interference fringes caused by reflection at the various interfaces. This phenomenon is less evident at higher temperatures (≥ 900 °C) since the thickness of the films shrinks due to thermal densification. Interestingly, $T^H D^H_2$ films are more transparent in a range of 200–350 nm, compared to the TEB- $T^H D^H_2$ films (Fig. 6b). The higher absorbance of the B-containing film (TEB- $T^H D^H_2$) in this wavelength range could be due to the presence of B–C bonds. However, a more detailed EPR and NMR study on corresponding SiBOC powders to understand the effect of the defect states on optical properties is in progress.

5. External quantum efficiency measurements

Measurements of the photoluminescence quantum yield of thin film samples are problematic due to the difficulties in determining the angular distribution of the emission, their reflectivity, and absorbance. Usually, EQE measurements require calibrated integrating sphere and dedicated set-up. In this study, we use a simple method to measure the external quantum efficiency (EQE).

By calibrating the measurement set up with respect to a calibrated red LED, the spectrally integrated luminescence intensity emitted by the films under UV-photo-excitation is measured and converted into an emitted photon flux. The photon flux was corrected by the numerical aperture of the collecting system by assuming that the film is a lambertian point source. It is considered that the total absorbed power by the active thin film is equal to the total laser power incident on the sample (P_{laser}) minus the power transmitted by the sample, the power reflected by the sample and the power absorbed by the quartz substrate. These quantities are measured with a power-meter calibrated at 365 nm. Knowing the wavelength of the laser, the absorbed photon flux is deduced. The ratio between the emitted and the absorbed photon fluxes yields the EQE of the film.

Accordingly, the EQE of the TEB- $T^H D^H_2$ thin film annealed at 900 °C is calculated as 4%, which is comparable to $T^H D^H_2$ films [12]. In the calculation, the UV emission part of the PL peak was not included so the real value is surely higher than 4%, which is among the highest EQE values in Si based materials. We would like to emphasise the importance of the findings that the high efficiency from TEB- $T^H D^H_2$ films coupled with an unusual broad and tunable PL emission gives feasibility of efficient tunable silicon-based white light emitting sources fabricated by using a very simple process (sol-gel).

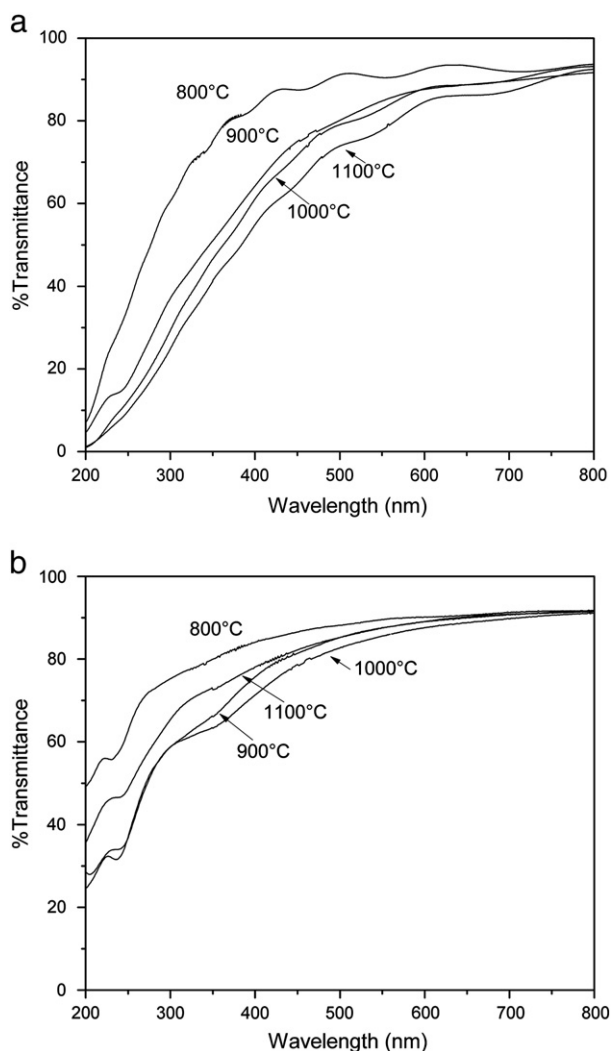


Fig. 6. UV-visible spectra of (a) TEB- $T^H D^H_2$ and (b) $T^H D^H_2$ films pyrolysed at 800–1100 °C.

6. Conclusion

SiBOC films were synthesized by controlled pyrolysis of sol–gel-derived precursors and have been structurally and optically characterized. It is shown that the addition of B in SiOC changes drastically the properties of the film with superior performances for light emitting applications. Very interestingly, the film undergoes a smaller thermal shrinkage compared to SiOC, which allows an easy processing or shaping of the film. In addition, the complex structure of the SiBOC film gives rise to a wide distribution of emitting centers. In detail, high efficient, strong broad-band tunable visible emission has been observed from SiBOC ceramic thin films. All these features make the SiBOC thin films very promising materials for phosphor and electroluminescence applications.

Acknowledgement

This research is supported by the European Community FP6 through MCRTN-019601, PolyCerNet. Gian Domenico Soraru wishes to dedicate this paper to the memory of his sister Maria Teresa Sorarù who passed away on January 8th, 2009.

References

- [1] P. Colombo, G. Mera, R. Riedel, G.D. Soraru, *J. Am. Ceram. Soc.* 93 (2010) 1.
- [2] G.M. Renlund, S. Prochazka, R.H. Doremus, *J. Mater. Res.* 6 (1991) 2716.
- [3] G.M. Renlund, S. Prochazka, R.H. Doremus, *J. Mater. Res.* 6 (1991) 2723.
- [4] C.G. Pantano, A.K. Singh, H. Zhang, *J. Sol–Gel Sci. Technol.* 14 (1999) 7.
- [5] S. Dirè, R. Ceccato, F. Babonneau, *J. Sol–Gel Sci. Technol.* 34 (2005) 53.
- [6] G.D. Sorarù, F. Babonneau, S. Maurina, J. Vicens, *J. Non-Cryst. Solids* 224 (1998) 173.
- [7] A. Saha, R. Raj, D.L. Williamson, *J. Am. Ceram. Soc.* 89 (2006) 2188.
- [8] I. Menapace, G. Mera, R. Riedel, E. Ermen, R.-A. Eichel, A. Pauletti, G.A. Appleby, *J. Mater. Sci.* 43 (2008) 5790.
- [9] L. Ferraioli, D. Ahn, A. Saha, L. Pavesi, R. Raj, *J. Am. Ceram. Soc.* 91 (2008) 2422.
- [10] G.D. Sorarù, S. Modena, P. Bettotti, G. Das, G. Mariotto, L. Pavesi, *Appl. Phys. Lett.* 83 (2003) 749.
- [11] J.C. Pivin, M. Sendova-Vassileva, P. Colombo, A. Martucci, *Mater. Sci. Eng.* B69–70 (2000) 574.
- [12] A. Karakuscu, R. Guider, L. Pavesi, G.D. Sorarù, *J. Am. Ceram. Soc.* 92 (2009) 2969.
- [13] G. Das, L. Ferraioli, P. Bettotti, F. De Angelis, G. Mariotto, L. Pavesi, E. Di Fabrizio, G. D. Soraru, *Thin Solid Films* 516 (2008) 6804.
- [14] M.A. Schiavon, C. Gervais, F. Babonneau, G.D. Soraru, *J. Am. Ceram. Soc.* 87 (2004) 203.
- [15] R. Pena-Alonso, G. Mariotto, C. Gervais, F. Babonneau, G.D. Soraru, *Chem. Mater.* 19 (2007) 5694.
- [16] G.D. Sorarù, G. D'Andrea, R. Camprostrini, F. Babonneau, G. Mariotto, *J. Am. Ceram. Soc.* 78 (1995) 379.
- [17] A. Karakuscu, R. Guider, L. Pavesi, G.D. Sorarù, in: S. Mathur, M. Singh (Eds.), *Nanostructured Materials and Nanotechnology II, Ceramic Engineering and Science Proceedings*, vol. 29, John Wiley & Sons, Inc., NJ, 2008, p. 85.
- [18] M.A. Villegas, J.M. Fernández Navarro, *J. Mater. Sci.* 23 (1988) 2464.
- [19] G. Das, P. Bettotti, L. Ferraioli, R. Raj, G. Mariotto, L. Pavesi, G.D. Soraru, *Vib. Spectrosc.* 45 (2007) 61.
- [20] A. Kasgoz, T. Misono, Y. Abe, *J. Polym. Sci. A Polym. Chem.* 32 (1994) 1049.
- [21] G.D. Sorarù, R. Camprostrini, S. Maurina, F. Babonneau, *J. Am. Ceram. Soc.* 80 (1997) 999.
- [22] G.D. Sorarù, F. Babonneau, J.D. Mackenzie, *J. Mater. Sci.* 25 (1990) 3886.
- [23] C. Gervais, F. Babonneau, N. Dallabonna, G.D. Soraru, *J. Am. Ceram. Soc.* 84 (2001) 2160.